JACS
JOURNAL OF THE AMERICAN CHEMICAL SOCIETY

Article

pubs.acs.org/JACS

Open Access on 04/17/2015

Discovery of Amphipathic Dynorphin A Analogues to Inhibit the Neuroexcitatory Effects of Dynorphin A through Bradykinin Receptors in the Spinal Cord

Yeon Sun Lee,[†] Dhanasekaran Muthu,[†] Sara M. Hall,[†] Cyf Ramos-Colon,[†] David Rankin,[‡] Jackie Hu,[‡] Alexander J. Sandweiss,[‡] Milena De Felice,[‡] Jennifer Yanhua Xie,[‡] Todd W. Vanderah,[‡] Frank Porreca,[‡] Josephine Lai,[‡] and Victor J. Hruby*[,†]

[†]Department of Chemistry and Biochemistry and [‡]Department of Pharmacology, The University of Arizona, Tucson, Arizona 85721, United States

Supporting Information

ABSTRACT: We hypothesized that under chronic pain conditions, up-regulated dynorphin A (Dyn A) interacts with bradykinin receptors (BRs) in the spinal cord to promote hyperalgesia through an excitatory effect, which is opposite to the well-known inhibitory effect of opioid receptors. Considering the structural dissimilarity between Dyn A and endogenous BR ligands, bradykinin (BK) and kallidin (KD), this interaction could not be predicted, but it allowed us to discover a potential neuroexcitatory target. Well-known BR ligands, BK, [des-Arg^{10}, Leu^{9}]-kallidin (DALKD), and HOE140 showed different binding profiles at rat brain BRs than that previously reported. These results suggest that neuronal BRs in the rat central nervous system (CNS) may be pharmacologically distinct from those previously defined in non-neuronal tissues. Systematic structure−activity relationship (SAR) study at the rat brain BRs was performed, and as a result, a new key structural feature of Dyn A for BR recognition was identified: amphipathicity. NMR studies of two lead ligands, Dyn A-(4−11) **7** and [des-Arg^{7}]-Dyn A-(4−11) **14**, which showed the same high binding affinity, confirmed that the Arg residue in position 7, which is known to be crucial for Dyn A's biological activity, is not necessary, and that a type I β-turn structure at the C-terminal part of both ligands plays an important role in retaining good binding affinities at the BRs. Our lead ligand **14** blocked Dyn A-(2−13) **10**-induced hyperalgesic effects and motor impairment in in vivo assays using naïve rats. In a model of peripheral neuropathy, intrathecal (i.t.h.) administration of ligand **14** reversed thermal hyperalgesia and mechanical hypersensitivity in a dose-dependent manner in nerve-injured rats. Thus, ligand **14** may inhibit abnormal pain states by blocking the neuroexcitatory effects of enhanced levels of Dyn A, which are likely to be mediated by BRs in the spinal cord.

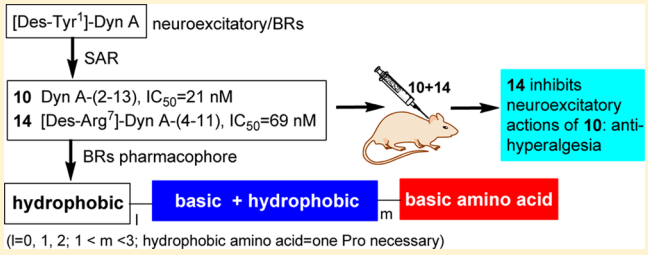

INTRODUCTION

Dynorphin A (Dyn A, Figure 1) is a known endogenous opioid peptide along with enkephalin and endorphin, and is characterized by its high affinity for mu (μ), delta (δ), and kappa (κ) opioid receptors. The high affinity of Dyn A for the opioid receptors is mainly due to the *N*-terminal tyrosine, because des-tyrosyl fragments show very low binding affinity at opioid receptors.[1] In vivo, Dyn A is degraded rapidly upon release to the des-tyrosyl analogue by aminopeptidases in the synapse to terminate Dyn A's agonist action at the opioid receptors.[2] Dyn A inhibits smooth muscle contractility, which is characteristic of opioid agonists and is blocked by naloxone. It is also well documented that Dyn A and its des-tyrosyl analogues can produce motor impairment, paralysis, and enhanced sensitivity to sensory stimuli.[3−7] These effects are not blocked by naloxone, and thus are nonopioid in nature.

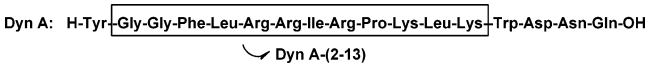

Figure 1. The structures of Dyn A and Dyn A-(2−13).

It has been proposed that after nerve injury, up-regulated Dyn A in the spinal cord may interact directly with spinal bradykinin receptors (BRs) to promote neuropathic pain.[8,9] Considering the lack of structural similarity between Dyn A and the endogenous ligands for the BRs, bradykinin (BK) and kallidin (KD), this interaction between Dyn A and BR could not be predicted but allowed us to identify a putative direct neuroexcitatory target. Here, we test the therapeutic potential of a pharmacological intervention of Dyn A at spinal BRs in chronic pain states by developing BR antagonists based on the prototypic structures of Dyn A.

Received: October 10, 2013
Published: April 17, 2014

   dx.doi.org/10.1021/ja501677q | *J. Am. Chem. Soc.* 2014, 136, 6608−6616

Table 1. Binding Affinities of Dyn A (H-Tyr[1]-Gly-Gly-Phe-Leu-Arg-Arg-Ile-Arg-Pro-Lys-Leu-Lys-Trp-Asp-Asn-Gln[17]-OH) Fragments and Dyn A-(4−11) Analogues at BRs in Rat Brain

		BR[a], [^{3}H]DALKD	
no.	ligand	log [IC_{50}][b]	IC_{50} (nM)
1	Dyn A-(3−6)	−6.02 ± 0.08	960
2	Dyn A-(3−7)	−5.01 ± 0.10	9800
3	Dyn A-(3−8)	−5.63 ± 0.27	2300
4	Dyn A-(3−9)	−6.11 ± 0.09	780
5	Dyn A-(3−10)	−6.09 ± 0.28	810
6	Dyn A-(3−11)	−6.88 ± 0.08	130
7	Dyn A-(4−11)	−6.86 ± 0.06	140
8	Dyn A-(5−11)	−6.55 ± 0.06	280
9	Dyn A-(5−12)	−5.15 ± 0.09	7100
10	Dyn A-(2−13)[c]	−6.78 ± 0.09	170
11	Dyn A-(3−13)	−6.50 ± 0.07	320
12	Dyn A-(4−13)	−6.41 ± 0.13	390
13	Dyn A-(5−13)	−6.33 ± 0.16	470
14	H-Phe-Leu-Arg-Ile-Arg-Pro-Lys-OH[c]	−6.71 ± 0.11	190
15	H-Phe-Leu-Arg-Arg-Ile-Arg-Pro-Lys-NH_2	−5.19 ± 0.20	6500
16	Ac- Phe-Leu-Arg-Ile-Arg-Pro-Lys-OH	−6.92 ± 0.28	120
17	Ac- Phe-Leu-Arg-Ile-Arg-Pro-DLys-OH	−6.20 ± 0.15	630
18	Ac-DPhe-Leu-Arg-Ile-Arg-Pro-Lys-OH	−6.44 ± 0.13	360
19	H-Phe-Leu-Arg-Ile-Arg-Pro-Arg-OH	−6.67 ± 0.15	210
20	Ac- Phe-Leu-Arg-Ile-Arg-Pro-Arg-OH	−6.86 ± 0.20	140
21	Ac-DPhe-Leu-Arg-Ile-Arg-Pro-Arg-OH	−6.84 ± 0.12	150
22	H-Phe-Nle-Arg-Nle-Arg-Pro-Arg-OH	−6.86 ± 0.12	140
23	Ac-Phe-Nle-Arg-Nle-Arg-Pro-Arg-OH	−6.85 ± 0.08	140
24	Ac-DPhe-Nle-Arg-Nle-Arg-Pro-Arg-OH	−6.70 ± 0.29	200
25	H-Phe-Ala-Arg-Ala-Arg-Pro-Arg-OH	−6.35 ± 0.18	450
26	H-Phe-Leu-Arg-Arg-Ile-Arg-Arg-Pro-Lys-OH	−6.96 ± 0.20	110
BK	H-Arg-Pro-Pro-Gly-Phe-Ser-Pro-Phe-Arg-OH[c]	−6.93 ± 0.08	120
DALKD	H-Arg-Pro-Pro-Gly-Phe-Ser-Pro-Leu-OH	−7.12 ± 0.11	76

[a]Competition assays were carried out at pH 7.4 using rat brain membranes. [b]Logarithmic values determined from the nonlinear regression analysis of data collected from at least two independent experiments in duplicate. [c]**10**: log [IC_{50}] = −7.29 ± 0.21, IC_{50} = 51 nM. **14**: log [IC_{50}] = −6.85 ± 0.04, IC_{50} = 140 nM. **BK**: log [IC_{50}] = −7.81 ± 0.17, IC_{50} = 15 nM at pH 6.8 in competition assays using [^{3}H]BK, and transfected HEK 293 cells expressing the human B2R.

RESULTS AND DISCUSSION

Structure−Activity Relationships (SAR) Study. The key step in the rational design of BR antagonists is to identify the pharmacophore of Dyn A that directly interacts with the BRs as an agonist and then to refine the structure for the binding site by examining the effects of different substituents to obtain an antagonist.[10] First, each amino acid at the *C*-terminal or *N*-terminal position of Dyn A-(2−13) (**10**), which has been reported to have neuroexcitatory nonopioid effects through BRs in the spinal cord,[1,7,8] was truncated in sequence and the resulting fragments were tested for their binding to BRs against [^{3}H][des-Arg[10],Leu[9]]-kallidin ([^{3}H]DALKD) or [^{3}H]BK in rat brain membranes. As a result, a key pharmacophore of Dyn A for the BRs was identified as well as distinct SAR (Table 1). Dyn A-(4−11) (**7**), which has the same range of binding affinity (IC_{50} = 140 nM) as **10** (IC_{50} = 170 nM), was identified as a good pharmacophore for the BRs. Also, the SAR results revealed that the BR recognition predominantly depends on the basicity of the *C*-terminal amino acid residue.

The Dyn A fragments **4**, **6**, and **13**, which have a *C*-terminal basic amino acid such as Lys or Arg, showed higher binding affinities than those fragments (**3**, **5**, and **9**) with a *C*-terminal hydrophobic amino acid such as Ile, Pro, or Leu. For example, Dyn A-(5−13) (**13**) showed moderate affinity (IC_{50} = 470 nM) at the receptor, and after truncation of a Lys residue at the *C*-terminus its affinity was reduced 15-fold (**9**, IC_{50} = 7100 nM). However, subsequent truncation of a Leu residue at the *C*-terminus recovered or even increased its binding to the receptor (**8**, IC_{50} = 280 nM). This distinct SAR at the *C*-terminus was maintained during the successive truncations of *C*-terminal residues, and this result confirmed the important role of a positive charge for the *C*-terminal amino acid residues in receptor recognition.

On the other hand, consecutive truncations of the *N*-terminal amino acid residues to position 4 did not affect their affinities to the receptor. The truncation of two amino acid residues, Gly and Phe, in **6** and **10** resulted in negligible reduction of the affinities to the receptor. These results suggest that the *N*-terminal part of the Dyn A is remote and thus not involved in binding to the BRs. This is an important feature of SAR to understand how Dyn A analogues recognize the receptor. The positive charge of the C-terminal basic amino acid residue may be mainly involved in electrostatic interactions with the receptor.

Further SAR studies on the minimum pharmacophore **7** were performed to distinguish the receptor interaction and to increase the potency and in vivo stability. Although two Arg residues at positions 6 and 7 have been known to be important for the biological activity of Dyn A,[11,12] on the basis of our primary SAR results and the amphipathic properties of Dyn A

dx.doi.org/10.1021/ja501677q | J. Am. Chem. Soc. 2014, 136, 6608−6616

structure, it did not seem to be necessary to retain two Arg residues for binding to BRs. Therefore, the Arg residue at position 7 was deleted, and interestingly the resulting ligand **14** retained high binding affinity (IC_{50} = 190 nM) to the BRs. The removal of the Arg residue at position 7 did not affect binding affinity at all. This is remarkable because in general, deleting one amino acid in the middle of a bioactive sequence typically causes significant topographical changes and a different biological profile.

As discussed earlier, the *C*-terminal basic amino acid residue plays an important role in BR recognition. If the receptor recognition is mainly through electrostatic interactions with positive charges of the side chain group of a basic amino acid residue, the amidation of a *C*-terminal acid group can be a useful modification to increase in vivo stability in the same range of binding affinity. For this purpose, the *C*-terminal acid was amidated in **15**, but the modified ligand had greatly reduced binding affinity (IC_{50} = 6500 nM). All other amidated ligands (see Supporting Information) exhibited very low binding affinities in the micromolar range, and this confirms the role of a *C*-terminal acid in the recognition of the BR.

In contrast, modifications of the *N*-terminal part had little effect on binding affinities. Acetylation of N^{α}-amino group in ligand **16** (IC_{50} = 120 nM), **20** (IC_{50} = 140 nM) and **23** (IC_{50} = 140 nM) retained good binding affinities in the same range as nonacetylated analogues. Even the inversion of chirality of the Phe residue from L to D did not reduce their binding affinities at the BR in **18** (IC_{50} = 360 nM), **21** (IC_{50} = 150 nM), and **24** (IC_{50} = 200 nM). On the other hand, the same modification at the *C*-terminus by D-Lys decreased its binding more than 10-fold in **17** (IC_{50} = 630 nM). However, thanks to the same basic property, the substitution of a Lys residue at the *C*-terminus with an Arg in ligands **19**–**24** was tolerated well to maintain the same high binding affinities as **14**, even with various modifications of the *N*-terminal position.

In order to identify the role of hydrophobic amino acids neighboring Arg residues, the Leu and Ile residues were replaced by an Ala residue, and the resulting ligand **25** had decreased binding affinity (IC_{50} = 450 nM). Even with the slight loss of affinity, this result suggests that hydrophobicity and size of the hydrophobic amino acid residues play a role in isolating basic amino acid residues. When the two Ala residues in **25** were replaced by two Nle, respectively, the modification recovered binding affinity (**22**, IC_{50} = 140 nM) to the same range as **19**. Further acetylation did not change the binding affinity in ligands **23** (IC_{50} = 140 nM) and **24** (IC_{50} = 200 nM). These results clarify SAR at the *N*-terminal part, where neither acetylation nor D-amino acid replacement affects binding affinities of **14**, **16**, and **18**.

Heterogeneity of Bradykinin 2 Receptors (B2Rs). Interestingly, the binding affinity of BK in the rat brain membrane using [^{3}H]BK (IC_{50} = 91 nM; log [IC_{50}] = −7.04 ± 0.11) or [^{3}H]DALKD (IC_{50} = 120 nM; log [IC_{50}] = −6.93 ± 0.08) is lower than that (nanomolar range) reported previously for the B2R, which is the predominant BR type constitutively expressed in all tissues.[13−16] On the other hand, DALKD, which has been defined as a bradykinin type 1 receptor (B1R) selective antagonist, binds to the BRs (IC_{50} = 130 nM; log [IC_{50}] = −6.90 ± 0.07 and IC_{50} = 76 nM; log [IC_{50}] = −7.12 ± 0.11 vs, [^{3}H]BK and [^{3}H]DALKD, respectively) in rat brain membranes in the same range as BK.[11,14] The B2R selective antagonist, HOE140, had very low affinity (IC_{50} > 10 000 nM) against [^{3}H]BK binding in rat brain membranes. These results from rat brain BR binding sites differ significantly from that using guinea pig ileum (GPI) where both BK and HOE140 had high affinity (IC_{50} = 3.5 nM and 0.43 nM, respectively) similar to that previously reported.[13−16] Thus, in the rat central nervous system, we may be targeting a neuronal BR that is pharmacologically distinct from that previously defined in non-neuronal tissues. Furthermore, this neuronal BR exhibits affinity for Dyn A in the nanomolar range.

For comparison, selected Dyn A ligands that showed good affinities at rat brain BRs were tested for their binding affinities in transfected human embryonic kidney (HEK) 293 cells expressing the human B2R or B1R. Ligands **10** (IC_{50} = 51 nM), **14** (IC_{50} = 140 nM), and other ligands (see Supporting Information) exhibited a similar range of binding affinities for the HEKB2R as for the rat brain BRs (Table 1). However, none of the Dyn A ligands showed affinities at the HEKB1R where their affinities are >10000 nM. These results suggest that Dyn A ligands are selective for B2R over B1R.

NMR Structures. As discussed earlier, the most important SAR result was that removal of the Arg residue at position 7 did not affect binding affinities. Therefore, for the comparison of topographical structures of [des-Arg^7]-Dyn A and Dyn A, ligands **7**, Dyn A-(4−11), and **14**, [des-Arg^7]-Dyn A-(4−11), were selected and tested for their conformations in membrane-like sodium dodecyl sulfate (SDS) micelles by ^{1}H 2D-NMR spectroscopy.[17] As G-protein coupled receptors (GPCRs) such as BRs have their binding sites close to the lipophilic transmembrane (TM) domains, their ligand−membrane interactions play an important role in biological activities.[18] The membrane can also promote ligand−receptor docking by stabilizing their secondary structural elements.[19,20] Therefore, for further insight into biological profiles it is crucial to identify the membrane-bound structures of the ligands in these circumstances. In nuclear Overhauser effect (NOE) summary (Figure 2), both ligands showed strong consecutive $d_{\alpha N}(i, i+1)$ with a break at the Pro residue due to the imide nature of the residue; i.e., the Pro residue lacks an amide proton. Similarly they also displayed sequential $d_{\beta N}(i, i+1)$ NOEs throughout the sequence. Apart from trivial NOEs, consecutive $d_{NN}(i, i+1)$ NOEs and a number of medium range $d_{\alpha N}(i, i+2)$ NOEs in the middle segment were observed. It is noteworthy to observe consecutive medium range NOEs for shorter linear peptides such as ligands **7** and **14**. These observations along with no α-helical signature NOEs such as $d_{\alpha N}(i, i+3)$, $d_{\alpha N}(i, i+4)$ strongly suggest both ligands fold into consecutive turns or a 3_{10}-type helical fold. The observation of similar NOE patterns in both ligands indicates that the removal of an Arg residue does not significantly affect the overall conformation of these ligands in a membrane environment.

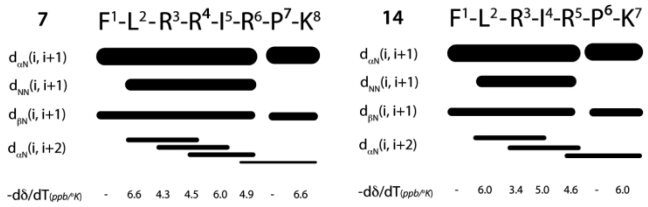

Figure 2. NOE summary and temperature coefficient values for **7** and **14**. The thickness of the line corresponds approximately to the intensity of NOE cross peaks.

$C^{\alpha}H$ chemical shifts are very sensitive to conformational structures, and their consecutive negative and positive deviations from random coil values indicate a helical fold and β-sheet structures, respectively.[21] Chemical shift index (CSI) plots (Figure 3) for both ligands **7** and **14** displayed a similar

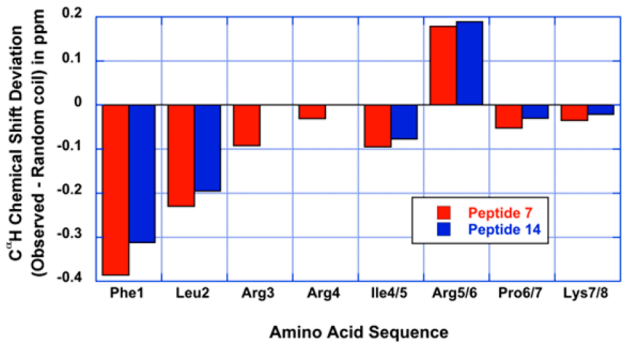

Figure 3. Chemical shift deviation of observed CαH values from the random coil values (CSI plot). It should be noted here that peptide **14** does not contain the Arg^4 residue.

trend. Although it is difficult to conclude simply on the basis of the CSI plot since **7** and **14** are very short peptides, the negative deviations from the random coil suggest a conformational space in the helical domain for both ligands. It could be either a β-turn structure or a 3_{10}-type helical structure. Simulated annealing molecular dynamics calculations were carried out in order to obtain three-dimensional structures. NMR-derived distance and dihedral angle constraints were applied in the calculations as described in the Supporting Information. The stereochemical quality for the final minimized structures was verified by the distribution of per-residue backbone dihedral angles (Phi and Psi) in the Ramachandran plot. The distribution of Phi and Psi angles for **14** is concentrated in only one region for all residues except the *C*-terminal Lys residue, suggesting that the conformational ensemble contains a single family of structures with conformational flexibility at the *C*-terminus around the Lys residue (Figure 4). A closer examination of dihedral values and their distribution in the Ramachandran plot identifies two consecutive type III β-turns (or a short 3_{10}-helix: type III β-turns and 3_{10}-helix have the same dihedral angle values) at the *N*-terminus, and a distorted type 1 β-turn at *C*-terminal region centered at Pro^7-Lys^8 in **7**. However, the removal of an Arg residue in **14** resulted in a single type III β-turn at the *N*-terminus and the same distorted type I β-turn at the *C*-terminus. The consecutive turn structure at the *N*-terminus in **7** may not be necessary for the B2R interactions considering the same range of binding affinities of **7** and **14**. Ramachandran plots of each amino acid for all the final hundred structures of **7** revealed semi rigid conformations for all the residues except for the Arg, or Arg and Lys residues where the Psi angle deviation is greater than 30 degrees from the average value. We suggest that the flexibility of the three basic amino acids in **14** could contribute to the receptor recognition by adapting the same conformation as **7**.

The NMR study showed that the two ligands, **7** and **14**, have the same distorted type 1 β-turn structure at the *C*-terminus, which is considered a key region for binding. This explains how the two ligands bind to the receptor with the same affinity even with a dissimilarity of structure at the *N*-terminus. As mentioned above, the *N*-terminal part does not play an

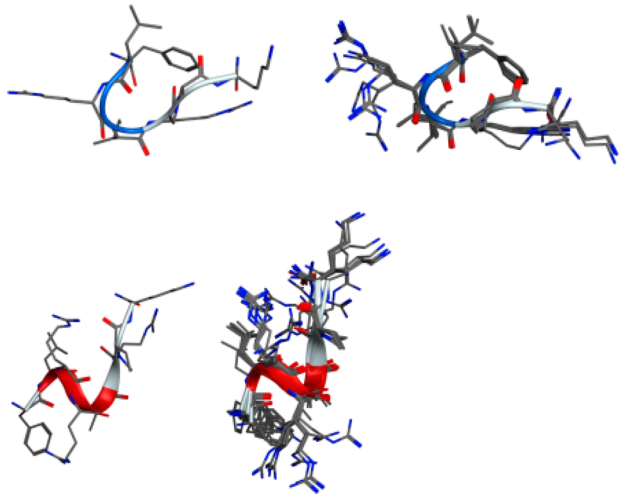

Figure 4. Lowest energy structure and overlay of 10 low energy structures of **7** (lower) and **14** (upper) from the simulated annealing molecular dynamics calculations. The hydrogen atoms are not shown for clarity. The ribbon diagram shows the secondary structure of the peptide. RMSD between structures is 2.013 Å (1.694 Å for **14**) when all the atoms are considered but is reduced significantly to 0.502 Å (0.155 Å for **7**) when only backbone atoms are considered.

important role in the receptor interactions and thus does not affect ligand binding. Also one Arg residue at position 3 of ligand **14** seems to be sufficient for receptor recognition similar to the two Arg residues in ligand **7**. In Figure 3, the Arg residue at positions **5** or **6** showed high positive deviations, which indicate the formation of β-sheet structures. When one more Arg residue was inserted between positions 6 and 7 in ligand **7**, the resulting ligand **26** retained nearly the same binding affinity (IC_{50} = 110 nM) at the receptor as **7** and **14**.

Binding Affinities and pH Sensitivity. It has been previously shown that the optimal binding conditions for the BR to its endogenous ligands, including BK, is at pH 6.8.[22] Thus, we also tested the effect of pH 6.8 on the ability of Dyn A analogues to bind to the BR in rat brain membranes (Table 2,

Table 2. Binding Affinities of Dyn A Analogues at BRs in Rat Brain at pH 6.8 or 7.4[a]

	[^{3}H]DALKD, pH 7.4		[^{3}H]DALKD, pH 6.8	
ligand	log [IC_{50}]	IC_{50} (nM)	log [IC_{50}]	IC_{50} (nM)
7	−6.86 ± 0.06	140	−7.16 ± 0.16	69
10	−6.78 ± 0.09	170	−7.67 ± 0.05	21
14	−6.71 ± 0.11	190	−7.16 ± 0.09	69
26	−6.96 ± 0.20	110	−7.13 ± 0.04	74
BK	−6.93 ± 0.08	120	−7.01 ± 0.05	98
DALKD	−7.12 ± 0.11	76	−6.98 ± 0.10	100

[a]Details described in Table 1.

Figure 5). These initial analyses found that the affinity for all 4 analogues selected was enhanced by 2 to 8 fold. Additional analyses shown in Table 3 demonstrate that other analogues also interact with the rat brain BR with affinities in the nanomolar range. These data validate the optimal binding conditions for the Dyn A analogues to be at pH 6.8, which is consistent with the binding conditions previously established for BRs.

Identification of Dyn A Pharmacophore for BRs. On the basis of the binding affinities of the three ligands **7**, **14**, and

dx.doi.org/10.1021/ja501677q | J. Am. Chem. Soc. 2014, 136, 6608−6616

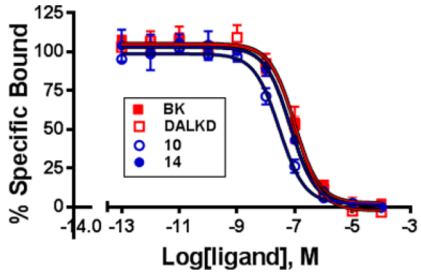

Figure 5. Inhibition of [^{3}H]DALKD binding to rat brain membrane at pH 6.8. Rat brain membrane was incubated with [^{3}H]DALKD and increasing concentrations of ligands. Data for each nonlinear regression analysis were collected from at least two independent experiments.

Table 3. Amphipathic Dyn A Analogues and Their Binding Affinities for BR in Rat Brain at pH 6.8[a]

		BR, [^{3}H]DALKD	
no.	structure	log [IC_{50}]	IC_{50} (nM)
27	H-Leu-Arg-Ile-Arg-Pro-Lys-Leu-Lys -OH	−7.52 ± 0.09	30
28	H-Nle-Lys-Nle-Lys-Pro-Lys-Nle-Lys-OH	−7.04 ± 0.10	91
29	H- Lys-Nle-Lys-Pro-Lys-Nle-Lys-OH	−7.07 ± 0.16	85
30	H-Nle-Lys-Pro-Lys-Nle-Lys-OH	−7.11 ± 0.14	78
31	H- Lys-Pro-Lys-Nle-Lys-OH	−6.64 ± 0.13	230
32	H- Arg-Pro-Lys-Leu-Lys-OH	−7.24 ± 0.12	58
33	H-Pro-Lys-Leu-Lys-OH	−6.68 ± 0.10	210

[a]Details described in Table 1.

26, it was considered that two neighboring basic amino acid residues are not necessary for BR recognition, and furthermore it was observed that in relatively longer length analogues such as ligand **27**, truncation of the Arg residue increased their binding affinities (log [IC_{50}] = −7.17 ± 0.10, IC_{50} = 68 nM at pH 7.4, cf. **13**) (Table 3). From the structure of ligand **27**, it is clear that the ligand consists of basic amino acids and hydrophobic amino acids possessing amphipathic properties and a Pro residue making a turn structure. This is similar to other ligands that show good binding affinities to the BR. Successive truncations of *N*-terminus and substitutions of a basic amino acid residue and hydrophobic amino acid residue with a Lys and Nle did not change their affinities. Analyzing the structure of all the ligands that showed good binding affinities at the BRs provides the following insight regarding the pharmacophore of Dyn A analogues for the rat BR in the CNS: It requires a basic amino acid residue such as a Lys and Arg at the *C*-terminus, combinations of basic amino acid residues and hydrophobic amino acid residues, and a Pro residue as a hydrophobic residue to make a turn structure. On the basis of the SAR results, the pharmacophore for the BR can be simplified as an amphipathic structure as shown below in Figure 6. Ligand **32**, which retained high binding affinity (IC_{50} = 58 nM) after successive truncation at the *N*-terminus, is

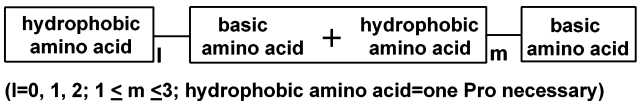

Figure 6. Pharmacophore of Dyn A for BRs.

considered as a minimum pharmacophore to fulfill the structural requirement (l = 0, m = 2, one Pro). Together, it suggests that the BR recognition depends on the electrostatic interactions between positive charges of the ligand and negative charges of the BR, and thus to amplify the electrostatic interactions, the positive charges of the ligand should be allocated by making a proper topographical structure. This may be the role of hydrophobic amino acid residues including the Pro.

Off-Target Screening and Functional Assay. As shown in Figure 6, the pharmacophore of Dyn A for BRs represents a simple amphipathic structure. In order to ensure the specificity of the Dyn A analogues for the BR, lead ligands **14** and **32** were screened at 43 off-target receptors. While the screen was limited, the blinded analysis supports the notion that the ligands' interaction with BR is specific (see Supporting Information). We also tested selected Dyn A analogues for their binding to the three cloned opioid receptors ([^{3}H]-DAMGO, ([^{3}H]deltorphin, and [^{3}H]U69,593 for the rat mu opioid receptor (rMOR), human delta opioid receptor (hDOR), and human kappa opioid receptor (hKOR), respectively). No ligand showed affinities for the μ and δ opioid receptors but ligands **10**−**13**, which include a longer *N*-terminus part, exhibited low affinities (**10**, K_i = 560 nM; **11**, K_i = 2400 nM; **13**, K_i = 2200 nM) at the κ opioid receptor (n = 2). However, our lead ligands, **14** and **32**, did not exhibit affinity at the κ opioid receptor (K_i > 10 000 nM, n = 2). These results show that our strategies have successfully differentiated opioid and nonopioid functions.

To determine the functional activity of ligand **14**, we tested its ability to stimulate the hydrolysis of [^{3}H]inositol phosphates in transfected HEK 293 cells expressing the human B2R. This bioassay measures the production of the intracellular second messenger, inositol triphosphate, which has been defined as the primary signal produced upon the activation of B2R by BK.[23] In the HEKB2R cells (Figure 7), BK stimulated the production of

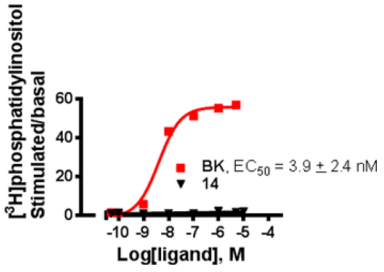

Figure 7. Phosphatidylinositol (PI) assay. The effect of test drug on production of [^{3}H]inositol phosphates was expressed as a ratio of stimulated over basal activity defined as the amount detected in the absence of test drug. EC_{50}: concentration at 50% of maximal stimulation. Data are representative of 3 independent experiments.

[^{3}H]inositol phosphates with an EC_{50} of 3.9 ± 2.4 nM. Ligand **14**, in contrast, showed no stimulation up to a dose of 10 μM. Also, there was no overt cell death observed in ligand **14** up to 10 μM.

In Vivo Assay: Toxic and Hyperalgesic Effects. The nontoxic effect of ligand **14** was also demonstrated by in vivo rotarod and hindlimb tests using naïve rats (Figure 8). In the rotarod test, intrathecal (i.th.) administrations (3 nmol) of **14** retained the similar latencies as vehicle and **10**. In the hindlimb test, i.th. administration of **14** did not show any motor

dx.doi.org/10.1021/ja501677q | J. Am. Chem. Soc. 2014, 136, 6608−6616

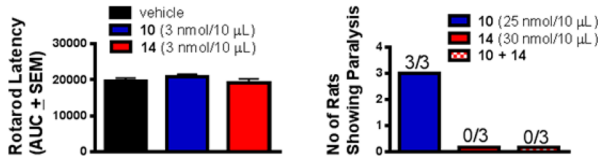

Figure 8. Rotarod (left) and Hindlimb (right) tests by i.th. administration of **10** or/and **14** in naïve rats.

impairments at a high dose (30 nmol), but **10** (25 nmol, i.th) induced paralysis that occurred within a few minutes post-injection and lasted for 30 to 40 min. In addition, pretreatment of **14** (30 nmol, i.th.) completely blocked ligand **10** (25 nmol, i.th.)-induced paralysis, suggesting that ligand **14** may inhibit Dyn A's excitatory effects in vivo.

To evaluate the hyperalgesic effects of **10** and **14**, radiant heat and von Frey filaments tests were performed in naïve rats (Figure 9). Paw withdrawal latencies and thresholds of all

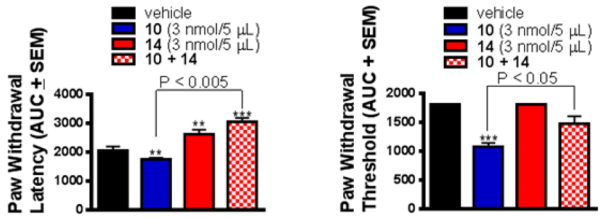

Figure 9. Effects of ligand **10** or/and **14** on thermal hyperalgesia (left, radiant heat test) and tactile hypersensitivity (right, von Frey test) 2 h after i.th. administration in naïve rats. Ligand **10** decreased thermal latency and tactile thresholds after i.th. administration. Ligand **14** blocked ligand **10**-induced thermal hyperalgesia and tactile hypersensitivity after coadministration. Statistical significance was determined by 95% confidence interval (*P < 0.05, **P < 0.01, ***P < 0.001 vs vehicle; $n \geq 6$).

animals were 18.7 ± 0.6 s and 15 ± 0 g, respectively. As expected, i.th. administration (3 nmol/5 μL) of ligand **10** reduced these values to 11.4 ± 1.0 s and 7.3 ± 1.0 g in 1 h, demonstrating thermal hyperalgesia (paw withdrawal latency: area under curve (AUC) ± SEM = 2067 ± 137 in 2 h) and mechanical hypersensitivity (paw withdrawal threshold: AUC ± SEM = 1074 ± 68 in 2 h). In contrast, administration of **14** increased latency of paw withdrawal from a heat source when compared with vehicle control, an effect that is defined as analgesic (Figure 9, left panel). **14** did not alter mechanical sensitivity (Figure 9, right panel). Coadministration of **10** and **14** prevented the hyperlalgegia induced by **10** when given alone. These data suggest that ligand **14** can effectively block ligand **10**, to induce abnormal pain states in vivo, presumably mediated by spinal BRs as an antagonist.

Thermal and tactile hypersensitivities were also assessed in rats that had received unilateral L_5/L_6 spinal nerve ligation (SNL) injury (Figure 10). Before injury, paw withdrawal latencies and thresholds of all animals were between 19.3−20.9 s and 15 g, respectively. SNL injury reduced these values to 8.6−11.3 s and 2.2−2.9 g, respectively, indicating abnormal sensitivities to thermal and tactile stimuli in the injured hind paw. Injured animals treated with ligand **14** showed antihyperalgesic effects in both tests in a dose dependent manner in 2 h. The greatest antihyperalgesic effects occurred at the highest dose of 3 nmol/10 μL in both tests.

The ability of **14** to reverse abnormal pain states in this model of neuropathy underscores the potential role of spinal

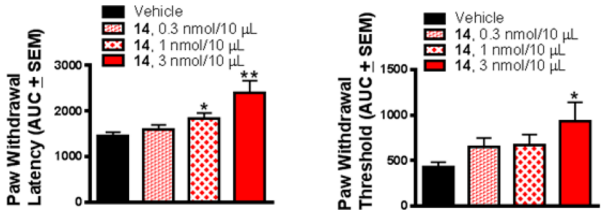

Figure 10. Dose-dependent reversal of thermal hyperalgesia (left, radiant heat test) and tactile hypersensitivity (right, von Frey test) using varying doses of **14** (i.th.) in L_5/L_6 SNL-operated male SD rats. Statistical significance was determined by 95% confidence interval (*P < 0.05, **P < 0.01 vs vehicle; $n \geq 6$).

BRs as a therapeutic target for neuropathic pain. **14** is a structure derived from Dyn A's interaction at the BRs. Together with our previous studies characterizing the role of spinal Dyn A in neuropathic pain, the results of the present study not only support a structural basis for Dyn A's actions at the spinal BRs to promote pain, but also show that it is possible to develop antagonists like **14** that target CNS BRs for therapy.

Peripheral Effects: Paw Edema and Plasma Extravasation. Local administration of **14** had no effect on BK-induced paw edema and plasma extravasation (Figure 11).

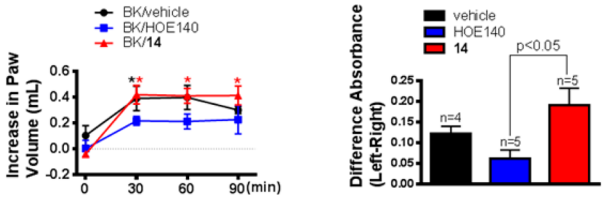

Figure 11. Effect of i.pl. injection of BK, given alone or in combination with HOE140 or 14 on paw edema (left) and plasma extravasation (right). Values shown represent the differences between volumes (mL) of vehicle and drug combination (BK/vehicle, BK/HOE140, and BK/14) paws (left, *P < 0.05 vs vehicle) and the difference absorbance (percent) of two hind paws (one vehicle only, the other BK/vehicle, BK/HOE140, and BK/14) at 620 nm by the content of Evans Blue dye (right).

Intraplantar (i.pl.) injection of BK (10 nmol) induced robust paw swelling and edema that peaked at 30 min postdose. The paw volume difference between the ipsi- and contralateral hind paws increased from 0.03 ± 0.09 mL (baseline) to 0.43 ± 0.08, 0.35 ± 0.08 and 0.23 ± 0.07 mL at 30, 60, and 90 min postdose, respectively. As expected, coadministration of a B2R antagonist, HOE140 (10 nmol, i.pl.), reduced the BK-induced paw volume increase to 0.22 ± 0.03 mL at 30 min postdose by 50%. In contrast, **14** (10 nmol, i.pl.) had no effect on paw edema with the same degree of paw volume increase (0.42 ± 0.07 mL at 30 min postdose) as that of BK alone. The same trend of effects was also observed in a plasma extravasation test. Coadministration of BK with **14** did not affect the BK-induced plasma extravasation, although HOE140 at this concentration was effective in reducing the extravasation on its own. This result suggests that our lead ligand **14** does not inhibit BK's action at the peripheral BRs, and therefore there will be little impact on the BK's cardiovascular function at the region. Paw edema and plasma extravasation tests show the possibility of ligand **14** as a drug candidate to block hyperalgesia in chronic pain states without serious cardiovascular side effects.

dx.doi.org/10.1021/ja501677q | J. Am. Chem. Soc. 2014, 136, 6608−6616

CONCLUSIONS

We have discovered a lead ligand **14** for CNS BRs and the human B2R through a systematic SAR study on Dyn A. Further modification of the lead ligand asserted the key structural features of the BR pharmacophore: amphipathicity. NMR study of two ligands **7** (Dyn A-(4−11)) and **14** ([des-Arg^7]-Dyn A-(4−11)) showed the same distorted type 1 β-turn structure at the *C*-terminus, a key region for the binding. Considering the pH dependence of the ligand's binding affinities, the BR recognitions seem to correlate with the electrostatic interactions between Dyn and BRs and thus for the optimization of their interactions, allocation of positive charges in ligands may be critical.

Ligand **14** inhibited ligand **10**-induced thermal and mechanical hyperalgesia in naïve animals. In nerve injured animals, ligand **14** blocked thermal and mechanical hypersensitivity in a dose-dependent manner. At high dose, ligand **10** showed serious motor impairment in vivo. In contrast, **14** did not show any toxicity, and motor impairment and furthermore blocked ligand **10**-induced paralysis in vivo. These in vivo activities of ligand **14** may be localized in the CNS, since there is no peripheral activity of ligand **14** shown in the paw edema and plasma extravasation tests. As we predicted, ligand **14** inhibits the actions of endogenous Dyn A's fragment, Dyn A-(2−13), resulting in antihyperalgesic effects in the CNS. This work further supports our hypothesis that the actions of spinal Dyn A at BRs underlie pathological pain states. These results also demonstrate that ligand **14** has the therapeutic potential for chronic pain states via a novel mechanism of BRs in the CNS.

EXPERIMENTAL SECTION

Synthesis. Dyn A analogues were synthesized by standard solid phase peptide synthesis using N^{α}-Fmoc-chemistry (Fmoc = 9-fluorenylcarboxy) on amino acid preloaded Wang resin (100−200 mesh, Novabiochem) in high yields (overall yield >40%), except for the analogues with a Pro residue at the *C*-terminus. Because of serious side reactions of Pro on the resin, Chlorotrityl resin (200−400 mesh, 1% DVB, Novabiochem) was used as an alternative.[24] Coupling was performed using 3 equiv 2-(1*H*-benzotriazole-1-yl)-1,1,3,3-tetramethylaminium hexafluorophosphate (HBTU)/3 equiv *N*-hydroxybenzotriazole (HOBt)/6 equiv diisopropylethylamine (DIPEA) in *N*,*N*-dimethylformamide (DMF) for 1 h at rt, and N^{α}-Fmoc-group was deprotected by 20% piperidine in DMF for 20 min at rt. In most cases, crude peptides were obtained by cleavage using a 95% trifluoroacetic acid (TFA) solution containing 2.5% triisopropylsilane (TIS) and 2.5% water for 3 h in high purity (70−90%) and could be isolated with more than 97% purity by preparative reverse phase high performance liquid chromatography (RP-HPLC) using gradient (10−40% acetonitrile in water containing 0.1% TFA in 15 min) in a short time (<15 min) because of their hydrophilic characters (refer to aLogPs in Supporting Information). The purified Dyn A analogues were validated by analytical RP-HPLC and high resolution mass spectroscopy in positive ion mode.

NMR Spectroscopy Methods. NMR studies of ligands **7** and **14** in SDS micelles were performed on a Bruker DRX600 (600 MHz) at 25 °C and at pH 5.5. Peptide concentrations for the NMR experiments were 5.8 mM and 6.1 mM for **7** and **14**, respectively. The micelle samples were prepared by dissolving the peptides and 50 equiv of perdeuterated SDS in 0.6 mL of acetate buffer (10 mM) containing 10% D_2O. The pH of each sample was adjusted to 5.5 by using DCl or NaOD as necessary. Deuterated 3-(trimethylsilyl)propionic acid (TSP) was added as an internal standard for referencing. Two-dimensional nuclear Overhauser enhancement spectroscopy (NOESY) and total correlated spectroscopy (TOCSY) (Supporting Information) were acquired using standard pulse sequences and processed using XWINNMR (Bruker, Inc.) and FELIX2000 (Accelrys, Inc., San Diego, CA). Mixing times for TOCSY and NOESY spectrum were 60 and 300 ms, respectively. All experiments were 750 increments in t1, 16, or 32 scans each, 1.5 s relaxation delay, size 2 or 4K, and the spectral processing was with shifted sine bell window multiplications in both dimensions. The water suppression was achieved by using WATERGATE pulse sequence. Coupling constants ($^3J_{\alpha H\text{-}NH}$) were measured from double quantum filtered correlation spectroscopy (DQF-COSY) experiments.

Structure Calculation Methods. Distance constraints for the structure calculation were obtained from integral volumes of the NOESY peaks. The NOE integral volumes were classified into strong, medium, and weak with 3.0, 4.0, and 5.0 Å as upper bound distance. Molecular dynamics simulation was done with the INSIGHT/DISCOVER package (Accelrys, Inc., San Diego, CA) with consistent valency force field (CVFF). All calculations were done in vacuo. A distance dependent dielectric constant (2.5r where r is the distance in Å) was used. All peptide bonds were constrained to *trans* conformation by a 100 kcal/mol energetic penalty. Distance restraints with a force constant of 25 kcal/mol were applied in the form of a flat-bottom potential well with a common lower bound of 1.8 Å and an upper bound of 3.0, 4.0, and 5.0 Å, respectively, in accordance with observed weak, moderate, or strong NOE intensities. Only the distance restraints from inter-residue NOEs were included in the calculation. Dihedral angle restraints based on $C_{\alpha}H$ CSI were imposed on the residues displaying negative deviation. Thus, for a CSI > −0.10 ppm, the ϕ and ψ restraints were in the range −90° to −30° and −60° to 0°, respectively, while for a CSI ≤ −0.10 ppm, the corresponding ranges were −150° to −30° for ϕ and −90° to 150° for ψ.

Radioligand Competition Binding Assays. Binding affinities of Dyn A analogues at the BRs were determined by radioligand competition analysis using [^{3}H]DALKD or [^{3}H]BK in rat brain membranes or in transfected HEK 293 cells expressing the human B2R. Crude rat brain membranes were pelleted and resuspended in 50 mM Tris buffer containing 50 μg/mL bacitracin, 10 μM captopril, 100 μM PMSF, and 5 mg/mL bovine serum albumin (BSA). Ten concentrations of a test compound were each incubated with 50 μg of membranes and [^{3}H]DALKD (1 nM, 76.0 Ci/mmol) or [^{3}H]BK (1 nM, 85.4 Ci/mmol) at 25 °C for 2 h. Nonspecific binding was defined by that in the presence of 10 μM KD in all assays. Reactions were terminated by rapid filtration through Whatman GF/B filters presoaked in 1% polyethylenimine, followed with four washes of 2 mL each of cold saline. Radioactivity was determined by liquid scintillation counting in a Beckman LS5000 TD. Data were analyzed by nonlinear least-squares analysis using GraphPad Prism 4. Logarithmic values were determined from nonlinear regression analysis of data collected from at least two independent experiments.

Functional Assays. Phosphatidylinositol (PI) assays were performed using [^{3}H]inositol phosphates tracer growth media (myo tritium inositol) in poly-D-Lys-coated cell culture plates, and the method used to measure the accumulation of [^{3}H]inositol phosphates was according to that described earlier with additional wash with water, 5 mM sodium tetraborate/60 mM sodium formate before elution with 0.2 mM ammonium formate/0.1 M formic acid through Biorad AG 1-X8 Resin.[25]

In Vivo Assays. The experiments were carried out using nonfasted male Sprague−Dawley rats (250−300g; Harlan; Indianapolis, IN) kept in a room controlled for temperature (22 ± 2 °C) and illumination (12 h on and 12 h off). All experiments were performed under a protocol approved by Institutional Animal Care and Use Committee (IACUC) of the University of Arizona, and in accordance with policies and guidelines for the care and use of laboratory animals as adopted by International Association for the Study of Pain (IASP) and the National Institutes of Health (NIH). Intrathecal (i.th.) catheterization was performed under ketamine/xylazine (80/12 mg/kg, i.p.) anesthesia. Some groups of rats were implanted with i.th. catheters (polyethylene 10, 7.8 cm) through atlanto-occipital membrane extended to the level of the lumbar spinal cord for drug administration. Animals were allowed to recover for 7 days. L_5/L_6 spinal nerve ligation (SNL) injury was induced as described by Chung and colleagues.[26]

dx.doi.org/10.1021/ja501677q | J. Am. Chem. Soc. 2014, 136, 6608−6616

Rotarod latencies, paw-withdrawal latencies, and paw-withdrawal thresholds were calculated and expressed as the mean AUC ± SEM in Graph Pad Prism 6 (GraphPad Software, La Jolla, CA). One-way analysis of variance (ANOVA) was performed in FlashCalc (University of Arizona, Tucson), and statistical significance achieved when $p \leq 0.05$.

Rotarod Test. Rats were trained to walk on an automated rotating rod (8 rev/min, Rotamex 4/8, Columbus Instrument, Columbus, OH) for maximal cutoff time of 180s.[27] Baseline values were recorded for each animal. Compounds were administered (i.th.) and assessment occurred every 20 min for the first 120 min. The rotarod latencies were recorded at each time point.

Motor Function and Paralysis. Paralysis was evaluated as flaccidity of the hind limbs following i.th. injection as previously reported by Spampinato and colleagues.[28] Drugs were injected in a volume of 5 μL, followed by a 1 μL air bubble and a 9 μL saline flush. Flaccidity of the hind limbs was measured for 2 h after drug administration.

Thermal Hypersensitivity Test (Radiant Heat). Thermal hypersensitivity was assessed using the rat plantar test (Ugo Basile, Italy) as described earlier.[27] Rats were allowed to acclimate within Plexiglas enclosures on a clear glass plate. A mobile radiant heat source (halogen bulb coupled to an infrared filter) was located under the glass plate and focused onto the hind paw. Paw withdrawal latencies were recorded in seconds. An automatic cut off point of 33 s was set to prevent tissue damage. The apparatus was calibrated to give a paw withdrawal latency of approximately 20 s on the uninjured paw. The radiant heat source was activated with a timer and focused onto the plantar surface of the hind paw.

Tactile Hypersensitivity Test (von Frey, Innocuous). The assessment of mechanical hypersensitivity consisted of measuring the withdrawal threshold of the paw ipsilateral to the site of nerve injury in response to probing with a series of calibrated von Frey filaments.[27] Each filament was applied perpendicularly to the plantar surface of the ligated paw of rats kept in suspended wire-mesh cages. Measurements were taken both before and after administration of drug or vehicle. The paw withdrawal threshold was determined by sequentially increasing and decreasing the stimulus strength ("up−down" method) analyzed using a Dixon nonparametric test16.

Measurement of Rat Paw Edema and Plasma Extravasation. Under ketamine/xylazine (80/12 mg/kg, i.p.) anesthesia animals received an injection of Evans Blue (30 mg/mL/kg, i.v.) via tail vein, and baseline paw volume for both hind paws was measured by use of a plethysmometer (Ugo Basile). Animals then received 0.1 mL i.pl. injections in one hind paw of normal saline (0.9% NaCl) containing BK either alone or mixed with HOE140 or **14** (10 nmol/paw each). The contralateral paw received 0.1 mL of saline and was used as a control. Edema was measured at several 30, 60, and 90 min after i.pl. injections and expressed in mL as the difference between the test and control paws. Three hours after BK injections, animals were sacrificed, and patches (10 × 5 mm) of the dorsal skin from both hind paws were collected. The skin patches were then incubated separately in Eppendorf tubes containing 1.8 mL of formamide at 60 °C water bath for 24 h to extract the dye. The tissue extraction was then centrifuged at 15 000 rpm for 15 min, and the supernatant was pipetted to a 96 well plate as triplicates and the absorbance was determined at 620 nm. The difference of the mean absorbance between the two hind paws of each rat was used to compare the degree of plasma extravasation in different treatment groups.

■ ASSOCIATED CONTENT

Ⓢ Supporting Information

Analytical data, binding affinity data, NMR spectroscopy. This material is available free of charge via the Internet at http://pubs.acs.org.

■ AUTHOR INFORMATION

Corresponding Author

hruby@email.arizona.edu

Notes

The authors declare no competing financial interest.

■ ACKNOWLEDGMENTS

We thank Jose Juan Ortiz Navarro, Ann Ngyuene, Alyssa Peake, Alice Cai, and Robert Kupp for their help in synthesis and bioassay of ligands. Off-target receptor screening was generously provided by the National Institute of Mental Health's Psychoactive Drug Screening Program, Contract # HHSN-271-2008-025C (NIMH PDSP). The NIMH PDSP is directed by Bryan L. Roth at the University of North Carolina at Chapel Hill and Project Officer Jamie Driscol at NIMH, Bethesda MD, USA. This work was supported by the U.S. Public Health Services, NIH, and NIDA (P01DA006284).

■ REFERENCES

(1) Lai, J.; Ossipov, M.; Vanderah, T. W.; Malan, T. P.; Porreca, F. *Mol. Interventions* **2001**, *1*, 160−167.
(2) Young, E. A.; Walker, J. M.; Houghten, R.; Akil, H. *Peptides* **1987**, *8*, 701−707.
(3) Faden, A. I.; Jacobs, T. P. *Br. J. Pharmacol.* **1984**, *81*, 271−276.
(4) Friederich, M. W.; Friederich, D. P.; Walker, J. M. *Peptides* **1987**, *8*, 837−840.
(5) Long, J. B.; Martinez-Arizala, A.; Echevarria, E. E.; Tidwell, R. E.; Holaday, J. W. *Eur. J. Pharm.* **1988**, *153*, 45−54.
(6) Walker, J. M.; Moises, H. C.; Coy, D. H.; Baldrighi, B.; Akil, H. *Science* **1982**, *218*, 1136−1138.
(7) Tang, Q.; Lynch, R. M.; Porreca, F.; Lai, J. *J. Neurophysiol.* **2000**, *83*, 2610−2615.
(8) Lai, J.; Luo, M. C.; Chen, Q.; Ma, S.; Gardell, L. R.; Ossipov, M.; Porreca, F. *Nat. Neurosci.* **2006**, *9*, 1534−1540.
(9) Altier, C.; Zamponi, G. W. *Nat. Neurosci.* **2006**, *9*, 1465−1467.
(10) Hruby, V. J. *Nat. Rev. Drug Discovery* **2002**, *1*, 847−858.
(11) Chavkin, C.; Goldstein, A. *Proc. Natl. Acad. Sci. U. S. A.* **1981**, *78*, 6543−6547.
(12) Turcotte, A.; Lalonde, J. M.; St-Pierre, S.; Lemaire, S. *Int. J. Pept. Protein Res.* **1984**, *23*, 361−367.
(13) Marceau, F.; Hess, J. F.; Bachvarov, D. R. *Pharm. Rev.* **1998**, *50*, 357−386.
(14) Innis, R. B.; Manning, D. C.; Stewart, J. M.; Snyder, S. H. *Proc. Natl. Acad. Sci. U. S. A.* **1981**, *78*, 2630−2634.
(15) Liebmann, C.; Bosse, R.; Escher, E. *Mol. Pharmacol.* **1994**, *46*, 949−956.
(16) Hess, J. F.; Borkowski, J. A.; Macneil, T.; Stonesifer, G. Y.; Fraher, J.; Strader, C. D.; Ransom, R. W. *Mol. Pharmacol.* **1993**, *45*, 1−8.
(17) Dhanasekaran, M.; Palian, M. M.; Alves, I.; Yeomans, L.; Keyari, C. M.; Davis, P.; Bilsky, E. J.; Egleton, R. D.; Yamamura, H. I.; Jacobsen, N. E.; Tollin, G.; Hruby, V. J.; Polt, R. *J. Am. Chem. Soc.* **2005**, *127*, 5435−5448.
(18) Berthold, M.; Bartfai, T. *Neurochem. Res.* **1997**, *22*, 1023−1031.
(19) Sargent, D. F.; Schwyzer, R. *Proc. Natl. Acad. Sci. U. S. A.* **1986**, *83*, 5774−5778.
(20) Palian, M. M.; Boguslavsky, V. I.; O'Brien, D. F.; Polt, R. *J. Am. Chem. Soc.* **2003**, *125*, 5823−5831.
(21) Wishart, D. D.; Bigam, C. G.; Holm, A.; Hodges, R. R.; Sykes, B. D. *J. Biomol. NMR* **1995**, *5*, 67−81.
(22) Regoli, D.; Barabe, J. *Pharmacol. Rev.* **1980**, *32*, 1−46.
(23) Grane*β*, A.; Adomeit, A.; Heinze, R.; Wetzker, R.; Liebmann, C. *J. Biol. Chem.* **1998**, *273*, 32016−32022.
(24) Chiva, C.; Vilaseca, M.; Giralt, E.; Albericio, F. *J. Pept. Sci.* **1999**, *5*, 131−140.
(25) Berridge, M. J.; Downes, C. P.; Hanley, M. R. *Biochem. J.* **1982**, *206*, 587−595.
(26) Chung, J. M.; Kim, S. H. *Pain* **1992**, *50*, 355−363.

(27) Largent-Milnes, T. M.; Yamamoto, T.; Nair, P.; Moulton, J. W.; Hruby, V. J.; Lai, J.; Porreca, F.; Vanderah, T. W. *Br. J. Pharmacol.* **2010**, *161*, 986−1001.
(28) Spampinato, S.; Romualdi, P.; Candeletti, S.; Cavicchini, E.; Ferri, S. *Pain* **1988**, *35*, 95−104.